**Supplemental Information**

to

# $SCF^{FBXO22}$ targets HDM2 for degradation and modulates breast cancer cell invasion and metastasis

Running Title: **Targeted degradation of HDM2 by $SCF^{FBXO22}$**

Jin Bai,[1,2,#,*] Kenneth Wu,[3,#] Meng-Han Cao,[1,4] Yingying Yang,[5] Yu Pan,[1,2] Hui Liu,[6] Yizhou He,[7] Yoko Itahana,[7] Lan Huang,[5] Jun-Nian Zheng,[1,2,4,*] Zhen-Qiang Pan[3,*]

[1]Jiangsu Key Laboratory of Biological Cancer, Cancer Institute
[2]Jiangsu Center for the Collaboration and Innovation of Cancer Biotherapy,
[4]Center of Clinical Oncology, Affiliated Hospital
[6]Department of Pathology
Xuzhou Medical University
Xuzhou 221002, Jiangsu Province, China

[3]Department of Oncological Sciences,
The Icahn School of Medicine at Mount Sinai
One Gustave L. Levy Place
New York, NY 10029-6574

[5]Departments of Physiology & Biophysics
University of California, Irvine, CA 92697

[7]Department of Radiation Oncology, Lineberger Comprehensive Cancer Center, the University of North Carolina at Chapel Hill, Chapel Hill, NC 27599, USA

[#]Equal contributors to this paper

[*]Corresponding Authors:
Zhen-Qiang Pan, Department of Oncological Sciences, Icahn School of Medicine at Mount Sinai, New York, NY 10029, USA. E-mail: zhen-qiang.pan@mssm.edu;
Jin Bai, Jiangsu Key Laboratory of Biological Cancer Therapy, Xuzhou Medical University, 84 West Huaihai Road, Xuzhou, 221002, Jiangsu Province, China.
E-mail: bj@xzhmu.edu.cn
Jun-Nian Zheng, Jiangsu Key Laboratory of Biological Cancer Therapy, Xuzhou Medical University, 84 West Huaihai Road, Xuzhou, 221002, Jiangsu Province, China.
E-mail: jnzheng@xzhmu.edu.cn

Key words: HDM2 abundance/E3 $SCF^{FBXO22}$/ Breast cancer metastasis

## Methods

### Plasmids

GST-HDM2 C464A contains C464A substitution, equivalent to MDM2 C462A mutation that eliminates RING E3 ligase activity[1]. Vector for expressing Flag-HDM2 in mammalian cells is described previously[2]. pEF-BOS-HA-FBXO22 was constructed to express HA-tagged FBXO22 with sequence as described previously[3]. pCMV-Ub-his6 is a gift of Dr. Serge Fuchs of University of Pennsylvania for the expression of 6XHis-tagged Ub in mammalian cells.

### Purification of GST-HDM2 C464A

pGEX-4T3-GST-HDM2 C464A[1] was transformed into BL21 (DE3). Bacterial growth, induction, extract preparation, and purification of GST-HDM2 C464A using glutathione beads were the same as described previously[3].

### Cells and animals

HeLa, HCT116 $p53^{-/-}$, HCT116 $p53^{+/+}$, and MCF-7 cells were cultured under standard conditions. Human breast cancer cell lines MDA-MB-231 and BT-549 were purchased from the Shanghai Institute of Biochemistry and Cell Biology, Chinese Academy of Sciences (Shanghai, China). MDA-MB-231 cells were cultured in Leibovitz' s L-15 Medium (Gibco, USA) supplemented with 10% fetal calf serum (Gibco, USA), BT-549 cells were cultured in RPMI 1640 Medium (Invitrogen, Shanghai, China) supplemented with 10% fetal calf serum. These two cells were both incubated in a 37°C humidified incubator with 5% $CO_2$.

Female BALB/c mice, 6 weeks old, were purchased from the Shanghai Laboratory Animal Center (Shanghai, China) for studies approved by the Animal Care Committee of Xuzhou Medical University.

**Isolation and identification of HDM2 E3 II**

The HDM2 E3 was isolated from HeLa extracts based on its ability to catalyze the ubiquitination of GST-HDM2 C464A, as monitored by immunoblot assays. HeLa cell extracts (11mg of protein/ml, 83ml) were prepared as described previously[3] and maintained in buffer A (25mM Tris [pH 7.5], 1mM EDTA, 0.01% Nonidet P-40, 10% glycerol, 1mM DTT, 0.1mM PMSF, 2μg/ml of antipain, and 2μg/ml of leupeptin) plus 25mM NaCl. The extracts were chromatographed through a Mono Q HR 10/10 (Amersham) in 2 batches. Bound protein was eluted by 160ml-gradient of 0.05-0.5M NaCl. Fractions #24-33 (around 150mM NaCl), containing HDM2 E3 II (Fig. 1A), were pooled (38ml, 5.19mg/ml). 20ml of this pool was diluted 6X with buffer A and up-loaded onto a Mono S (Amersham) in 3 batches. The flow through, containing HDM2 E3 II activity, were combined and concentrated using an Amicon Ultra concentrator (Millipore). The resulting fraction (1ml, 2.6mg/ml) was chromatographed by FPLC using a Superose 6 HR 10/30 gel filtration column (Amersham) in 5 batches. Peak activity fraction #27 (2ml; 2.2mg/ml) was used for glycerol gradient analysis and mass spectrometry. For glycerol gradient sedimentation, 200μl of Superose 6 fraction #27 was loaded on the top of 5ml of 15-35% of glycerol gradient containing buffer A plus 25mM NaCl and was centrifuged in an ultracentrifuge (Beckman) with a SW50.1 rotor at 45,000rpm for 20h.

To identify HDM2 E3 II, 1.8ml of Superose 6 fraction #27 was concentrated to 100μl, of which 37.5μl was subjected to 4-20% SDS-PAGE, followed by staining with Commassie

blue (see Fig. S3A). 28 excised gel slices, covering the entire lane as shown in Fig. S3A, were analyzed by mass spectrometry (MS/MS) as described previously[4].

***In vitro* ubiquitination**

Reaction mixture (10μl) contained 40mM $CrPO_4$, pH7.7, 1μg of creatine phosphokinase, 5mM $MgCl_2$, 2mM ATP, 0.6mM DTT, 0.1μg of purified GST-HDM2 C464A, 1.5μg of PK-HA-ubiquitin, 0.1μg of UbcH5c, E1 (15ng), and HeLa fraction or purified E3 in amount as indicated. After incubation at 37°C for 60 min, the reaction mixture was adsorbed to glutathione beads (15μl). Following washing 3 times with buffer B (15mM Tris-HCl, pH 7.4, 0.5M NaCl, 0.35% Nonidet P-40, 5mM EDTA, 5mM EGTA, 1mM PMSF, 2μg/ml of antipain, and 2μg/ml of leupeptin) and twice with buffer A plus 50mM NaCl, the bound proteins were eluted by SDS, separated by 4-20% SDS-PAGE, and visualized by immunoblot analysis using anti-HA antibody.

**siRNA transfection**

Small interfering RNAs (siRNAs) were purchased from GenePharma, Shanghai, China. siRNA sequences are as follows. For non-specific control: sense, 5'-UUCUCCGAACGUGUCACGUTT-3'; antisense, 5'-ACGUGACACGUUCGGAGATT-3'. For anti-FRBXO22 (1): sense, 5'-GGUGGGAGCCAGUAAUUAUTT-3'; antisense, 5'-AUAAUUACUGGCUCCCACCTT-3'. For anti-FRBXO22 (2): sense, 5'-GUUCGCAUCUUACCACAUATT-3'; antisense, 5'-UAUGUGGUAAGAUGCGAACTT-3'. For anti-FBXO31: sense, 5'-GAAGCUGCUUCACCGAUAUTT-3'; antisense, 5'-AUAUCGGUGAAGCAGCUUCTT-3'. For anti-RNF12: sense, 5'-GCAUCCAAUGAGUGAAAUUTT-3'; antisense, 5'-AAUUUCACUCAUUGGAUGCTT-3'. For anti-βTrCP: sense, 5'-GCACUUGCGUUUCAAUAAUTT-3'; antisense, 5'-

AUUAUUGAAACGCAAGUGCTT-3'. For anti-HDM2: sense, 5'-GCCUGCUUUACAUGUGCAATT-3'; antisense, 5'-UUGCACAUGUAAAGCAGGCTT-3'.

Unless indicated otherwise (Fig. S6A), anti-FBXO22 siRNA used in this work is the combination of anti-FBXO22 (1) and anti-FBXO22 (2) in 1:1 ratio. Cells were grown to 50% confluence prior to siRNA transfection using siLentFect Lipid Reagent (Bio-Rad, CA, USA) according to the manufacturer's protocol.

**Plasmid transfection and extract preparation**

Cells were grown to 90% confluence prior to transfection. Typically, plasmid (4μg) was transfected into cells using Lipofectamine 2000 transfection reagent (Invitrogen) following the manufacturer's instructions. 48h post-transfection, where indicated, cells were treated with MG132 (10μM) for 6h. Cells were lysed as described previously[5].

**Immunoprecipitation**

Extract proteins in amount as indicated were adsorbed to beads conjugated with antibody beads and the mixture was rocked for 2h at 4°C. After washing the beads 3 times with buffer B and twice with buffer A plus 50mM NaCl. The bound proteins were eluted by SDS, separated by 4-20% SDS-PAGE, and visualized by immunoblot analysis using indicated antibody.

**Immunoblot and antibodies**

Immunoblot analysis was performed as described previously[5]. The signals were detected and quantified by the Odyssey Infrared Imaging system (LI-COR). The following antibodies were purchased from: 1) Proteintech (rabbit anti-FBXO22, anti-FBXO31, anti-RNF12, anti-E-Cadherin, anti-N-Cadherin, and anti-GAPDH); 2) Cell

Signaling Technology (rabbit anti-MMP-2, anti-MMP-9, anti-βTrCP, and mouse anti-βactin); 3) Santa Cruz Biotechnology (mouse anti-Mdm2, anti-p53, and anti-Tubulin); or 4) LI-COR, NE, USA (Infrared IRDye-labeled secondary antibody). The blots were incubated with the indicated antibodies for 2h at room temperature.

**Cycloheximide chase**

The triple-negative MDA-MB-231 or BT-549 breast cancer cells were placed at a density of $10^6$ per 6cm diameter dish, allowed to adhere overnight. The cells were transfected with control siRNA or siRNA against FBXO22 at a concentration of 20nM. At 48h post-transfection, the treated cells were treated with cycloheximide (Sigma) at a final concentration of 50μg/ml and were harvested at the indicated time. Proteins were analyzed by immunoblot analyses using antibodies as specified, followed by quantification that is graphically presented.

***In vivo* ubiquitination**

MDA-MB-231 cells (2X10-cm dishes) were transfected with pCMV-ubiquitin-his6 and other vectors as specified. 48h post-transfection, cells were treated with MG132 (10μM) for 6h. Cells were lysed with 6M Guanidinium hydrochloride (GuHCl) in 0.1M Na-phosphate buffer, pH8.0 (6ml), followed by sonication for 1min. Ni-NTA (0.25ml, QIAGEN) was added to the lysates and the resulting mixture was rotated overnight at room temperature. The treated Ni-NTA was packed into a column (0.7cm, Econo BioRad), followed by sequential washes with the following solutions (2ml each): GuHCl, pH8.0; GuHCl, pH5.8; GuHCl, pH8.0; GuHCl (pH8.0) mixed with ProtBuffer (1:1) (ProtBuffer: 0.05M Na-phosphate, pH8.0, 0.1M KCl, 20% glucerol, and 0.2% NP40); GuHCl mixed with ProtBuffer (1:3); ProtBuffer; ProtBuffer plus 10mM imidazole. The bound protein was then eluted with 0.3M imidazole in ProtBuffer (1ml), followed by

concentration with the addition of 0.12ml of 100% TCA. After microfuge, the pellet was dissolved in cold acetone (0.5ml). Acetone was removed by microfuge. The dry pellet was re-suspended in 3X Laemmli (10μl) and 0.1M Na-phosphate pH8.0 (20μl). The eluted protein was separated by SDS-PAGE and analyzed by immunoblot analyses.

**Immunofluorescence**

For experiments shown in Fig. 3C, cells were fixed with 4% paraformaldehyde for 10min and washed with PBS three times (5min each), followed by treatment of Triton-X 100 (0.1%) at room temperature for 15min and then washing with PBS three times. BSA (2%) was added for incubation at room temperature for 20min. The resulting mixture was incubated with rabbit anti-FBXO22 (Proteintech) or mouse anti-Mdm2 (abcam) for overnight at 4°C. After washing with PBS three times, fluorescent second antibody was added for incubation at room temperature for 2h in a light-free environment. Following wash with PBS three times, the indicated samples were DAPI stained for 1min, then washed with PBS three times and sealed with nail polish. The fluorescent signals were detected by Laser confocal microscopy (LSM880, Deiss Company, Germany).

**Cell migration and invasion assays**

Cell migration and invasion assays were performed using modified two-chamber plates with a pore size of 8μm. The transwell filter coated with or without Matrigel (BD Biosciences, Mississauga, Canada) were used, respectively, for invasion or migration assay[6].

**Stable cell line generation**

First lentiviruses were generated by co-transfecting HEK293T cells with anti-FBXO22 (mouse) shRNA (5'-3',GGTGGGAGCCAGTAATTAT) or control shRNA (5'-3',

TTCTCCGAACGTGTCACGT) with the packaging plasmids (pMD2G and psPAX; GenePharma, Shanghai, China). 48h later the supernatant was collected, filtered (0.45-mm filters, Millipore, Temecula, CA, USA) and concentrated using Amicon Ultra centrifugal filters (Millipore 100,000 NMWL). The concentrated viruses were used to infect the 4T1 cells. 48h post infection the cells were selected with puromycin (2μg/ml, Santa Cruz) for two weeks, resulting in cell lines 4T1-luc-FBXO22-KD or 4T1-luc-Ctrl.

**Tail vein assay of metastasis**

The BALB/c nude mice were randomly divided into two groups: FBXO22-KD and control group, each consisted of 6 mice. The mice were injected intravenously with $5X10^5$ 4T1 cells in 100μl of phosphate-buffered saline (PBS) through tail vein. Bioluminescent imaging was regularly performed to monitor tumor burden *in vivo*, followed by end-of-study necropsy, and histopathological analysis of the lungs. After one month, the two groups of mice were sacrificed, their lungs were resected and fixed in 10% buffered formalin for histopathological analysis.

**Immunohistochemistry**

For experiments shown in Fig. 5D, after fixing the lungs in 10% buffered formalin, the resulting paraffin embedded tissues were subjected to further sectioning. The slides were incubated with a polyclonal rabbit anti-FBXO22 antibody (1:50 dilution; Proteintech, USA) or mouse anti-Mdm2 (1:100 dilution; Abcam, USA) at 4°C overnight. The resulting slides were treated with 3, 3′ -diaminobenzidine (DAB; Zhongshan Biotech, Beijing, China) to produce a brown precipitate. Non-immune serum was used as negative control. The levels of FBXO22 or MDM2 signals were quantified by IRS and shown graphically.

**Patient specimens and tissue microarray construction**

The collection of patient specimens and construction of the tissue microarray (TMA) have been previously described[7]. The study material consists of a series of 410 consecutive cases of primary breast carcinoma, from the First Affiliated Hospital of Nanjing Medical University, between 1996 and 2005. All these patients were treated with surgery only or with postoperative adjuvant therapy. The patients' clinicopathologic information including age at diagnosis, tumor size, histology grade, lymph node metastasis, ER status, PR status, HER2 status and p53 status was obtained from the archive of the pathology department and confirmed by the medical record of the hospital. The histologic grade was assessed using Bloom-Richardson classification. Five-year clinical follow-up results were available for 236 patients. The use of these tissue specimens was approved by the Ethics Committee of the Hospital. Also, these specimens and patient data were de-identified prior to use in our study.

**Immunohistochemistry of TMA**

Immunohistochemistry was carried out using a streptavidin-peroxidase (Sp) Kit (Zhongshan biotech, Beijing, China), as described previously[7]. The TMA slides were de-waxed at 60°C for 20min followed by three 5min washes with xylene. The tissues were then rehydrated by washing the slides for 5-min consecutively with 100%, 95%, 80% ethanol and finally with distilled water. The slides were then heated to 95°C for 30 min in 10mmol/L sodium citrate (pH 6.0) for antigen retrieval and then treated with 3% hydrogen peroxide for 1h to block the endogenous peroxidase activity. Subsequently the TMA slides were incubated with a polyclonal rabbit anti-FBXO22 antibody (1:50 dilution; Proteintech, USA) or mouse anti-Mdm2 (1:100 dilution; Abcam, USA) at 4°C overnight. The resulting slides were treated with 3, 3′ -diaminobenzidine (DAB; Zhongshan

Biotech, Beijing, China) to produce a brown precipitate. Non-immune serum was used as negative control.

**Evaluation of immune-staining**

FBXO22 or HDM2 staining was evaluated blindly and independently by two pathologists. Positive FBXO22 or HDM2 immuno-staining signal was observed predominantly in the cytoplasm. In some cases, FBXO22 or HDM2 signals were detected in both the cytoplasm and nucleus. The signals were quantified according to both the intensity and percentage of cells with positive staining. The FBXO22 or HDM2 staining intensity was scored 0 to 3 (0 = negative; 1 = weak; 2 = moderate; 3 = strong). The percentage of FBXO22-positive stained cells was also scored into four categories: 1 (0%-25%), 2 (26%-50%), 3 (51%-75%) and 4 (76%-100%). The level of FBXO22 or HDM2 staining was evaluated by IRS, which is calculated by multiplying the scores of staining intensity and the percentage of positive cells. Based on IRS, the FBXO22 or HDM2 staining pattern was categorized as negative (IRS: 0), weak (IRS: 1-3), moderate (IRS: 4-6) and strong (IRS: 8-12).

**Statistical analysis**

For the TMA, statistical analysis was performed with SPSS 20 software (SPSS, Inc, Chicago, IL). The association between FBXO22 staining and the clinicopathologic parameters of the breast cancer patients was evaluated by $\chi^2$ test. The Kaplan-Meier method and log-rank test were used to evaluate the correlation between FBXO22 expression and patient survival. Cox regression model was used for multivariate analysis. Data are expressed as the means ± SD. Two-factor analysis of variance

procedures and the Dunnett's t-test were used to assess differences within treatment groups. Differences were considered significant when $P < 0.05$.

For experiments shown in Fig. 6C, 407 breast cancer tissue samples were analyzed for expression of FBXO22 and HDM2 by IHC. The results were quantified and expressed by IRS. The correlation coefficients of FBXO22 and HDM2 were calculated by Spearman test.

**References**


1. Itahana K, et al. (2007) Targeted inactivation of Mdm2 RING finger E3 ubiquitin ligase activity in the mouse reveals mechanistic insights into p53 regulation. Cancer Cell. 12(4):355-66.
2. He Y, Tollini L, Kim TH, Itahana Y, Zhang Y. (2014) The anaphase-promoting complex/cyclosome is an E3 ubiquitin ligase for Mdm2. Cell Cycle. 13(13):2101-9.
3. Wu K, et al. (2003) DEN1 is a dual function protease capable of processing the C-terminus of Nedd8 and deconjugating hyper-neddylated CUL1. J Biol. Chem., 278, 28882-91
4. Fang L, et al. (2012) Mapping the protein interaction network of the human COP9 signalosome complex using a label-free QTAX strategy. Mol Cell Proteomics. 11(5): 138-47.
5. Wu, K, et al. (2000) The SCFHOS/**β**-TRCP-ROC1 E3 Ubiquitin Ligase Utilizes Two Distinct Domains within CUL1 for Substrate Targeting and Ubiquitin Ligation. Mol. Cell. Biol. 20, 1382-1393.
6. Bai J, et al. (2010) JWA regulates melanoma metastasis by integrin alphaVbeta3 signaling. Oncogene. 29(8):1227-37.
7. Bai J, et al. (2013) Cullin1 is a novel marker of poor prognosis and a potential therapeutic target in human breast cancer. Ann Oncol. 24(8):2016-22.
8. Siegel, L.M., and Monty, K.J. (1966). Determination of molecular weights and frictional ratios of proteins in impure systems by use of gel filtration and density gradient centrifugation. Application to crude preparations of sulfite and hydroxylamine reductases. Biochim. Biophys. Acta. 112(2), 346-62.
9. Li HL, Han L, Chen HR, Meng F, Liu QH, Pan ZQ, Bai J, Zheng JN. (2015) PinX1 serves as a potential prognostic indicator for clear cell renal cell carcinoma and

inhibits its invasion and metastasis by suppressing MMP-2 via NF-κB-dependent transcription. Oncotarget. 6(25):21406-20.

**Table S1:** FBXO22 expression & clinicopathologic characteristics of 410 breast cancer patients

| Variables | FBXO22 staining | | | |
|---|---|---|---|---|
| | Low (%) | High (%) | Total | *P* * |
| **Age** | | | | |
| ≤50 years | 84 (44.2) | 106 (55.8) | 190 | 0.842 |
| >50 years | 100 (45.5) | 120 (54.5) | 220 | |
| **Tumor size** | | | | |
| T1 (<2 cm) | 40 (51.9) | 37 (48.1) | 77 | 0.095 |
| T2 (2-5 cm) | 130 (44.4) | 163 (55.6) | 293 | |
| T3 (>5 cm) | 8 (28.6) | 20 (71.4) | 28 | |
| **Lymph node metastasis** | | | | |
| Negative | 77 (39.7) | 117 (60.3) | 194 | 0.001 |
| Positive | 106 (56.7) | 81 (43.3) | 187 | |
| **Histology grade** | | | | |
| I | 14 (38.9) | 22 (61.1) | 36 | 0.011 |
| II | 86 (41.7) | 120 (58.3) | 206 | |
| III | 44 (59.5) | 30 (40.5) | 74 | |
| **ER status** | | | | |
| Negative | 33 (44.6) | 41 (55.4) | 74 | 0.464 |
| Positive | 52 (39.1) | 81 (60.9) | 133 | |
| **PR status** | | | | |
| Negative | 42 (47.7) | 46 (52.3) | 88 | 0.116 |
| Positive | 43 (36.1) | 76 (63.9) | 119 | |
| **HER2 status** | | | | |
| Negative | 12 (57.1) | 9 (42.9) | 21 | 0.165 |
| Positive | 63 (40.6) | 92 (59.4) | 155 | |
| **p53 status** | | | | |
| Negative | 33 (39.8) | 50 (60.2) | 83 | 0.647 |
| Positive | 41 (44.1) | 52 (55.9) | 93 | |

* *P* values are from $\chi^2$ test.

Some cases were not available for the information.

**Table S2** Univariate Cox proportional regression analysis on 5-year overall and disease-specific survival of 410 breast cancer patients.

| Variable* | Overall survival | | | Disease-specific survival | | |
|---|---|---|---|---|---|---|
| | Hazard ratio | 95% CI† | *P** | Hazard ratio | 95% CI† | *P** |
| FBXO22 | | | | | | |
| Low | 1.000 | | 0.018 | 1.000 | | 0.021 |
| High | 0.604 | 0.398-0.918 | | 0.536 | 0.315-0.912 | |
| Age | | | | | | |
| ≤50 years | 1.000 | | 0.352 | 1.000 | | 0.053 |
| >50 years | 0.839 | 0.580-1.214 | | 0.587 | 0.342-1.007 | |
| Tumor size | | | | | | |
| ≤5 cm | 1.000 | | 0.016 | 1.000 | | 0.003 |
| >5 cm | 1.920 | 1.130-3.260 | | 2.877 | 1.448-5.717 | |
| Lymph node metastasis | | | | | | |
| Negative | 1.000 | | 0.000 | 1.000 | | 0.000 |
| positive | 3.616 | 2.292-5.704 | | 5.650 | 4.239-7.560 | |
| Histology Grade | | | | | | |
| I | 1.000 | | 0.020 | 1.000 | | 0.016 |
| II/III | 3.004 | 2.306-3.538 | | 2.711 | 1.657-3.183 | |

* *P* values are from Log-rank test.
† CI: confidence interval.

**Table S3** Multivariate Cox regression analysis on 5-year overall and disease-specific survival of 410 breast cancer patients.

| Variable* | Overall survival | | | Disease-specific survival | | |
|---|---|---|---|---|---|---|
| | Hazard ratio | 95% CI† | *P* | Hazard ratio | 95% CI | *P* |
| FBXO22 | 0.596 | 0.373 to 0.952 | 0.030 | 0.495 | 0.327 to 0.681 | 0.018 |
| Age | 0.915 | 0.567 to 1.475 | 0.714 | 0.697 | 0.378 to 1.286 | 0.249 |
| Tumor size | 2.563 | 1.770 to 3.176 | 0.007 | 2.796 | 1.821 to 3.929 | 0.003 |
| Lymph node metastasis | 5.715 | 2.800 to 11.662 | 0.000 | 6.852 | 4.888 to 8.958 | 0.000 |
| Histology Grade | 3.130 | 1.747 to 5.123 | 0.019 | 1.862 | 1.198 to 3.760 | 0.043 |

*Coding of variables: FBXO22 was coded as 1 (low), and 2 (high). Age was coded as 1 (≤50 years), and 2 (>50 years). Tumor size was coded as 1 (≤5 cm), and 2 (>5 cm). Lymph node metastasis was coded as 1 (negative), and 2 (positive). Histology grade was coded as 1 (I), and 2 (II and III).
† CI: confidence interval.

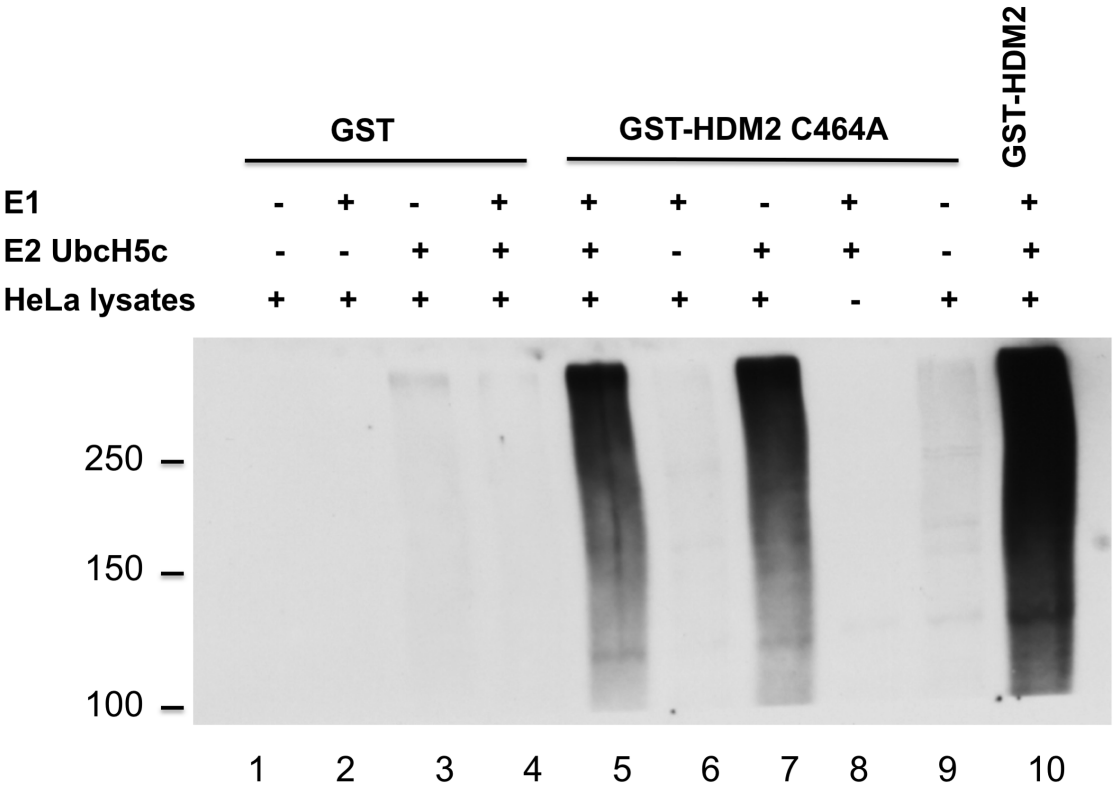


**Figure S1: Comparison of ubiquitination between GST, GST-HDM2, and GST-HDM2 C464A by HeLa cell lysates.** *In vitro* ubiquitination reaction was carried out in the presence of similar amounts of GST, GST-HDM2, or GST-HDM2 C464A, using a procedure similar to that described under Methods. Anti-Ub blot is shown. Note that GST-HDM2 exhibits ubiquitination activity at levels higher than that seen with GST-HDM2 C464A (compare lanes 5 and 10). This is because both intrinsic HDM2 RING-dependent auto-ubiquitination and extrinsic HeLa HDM2 E3 activities contribute to the ubiquitination of GST-HDM2. GST alone yielded barely detectable ubiquitination signal (lane 4).

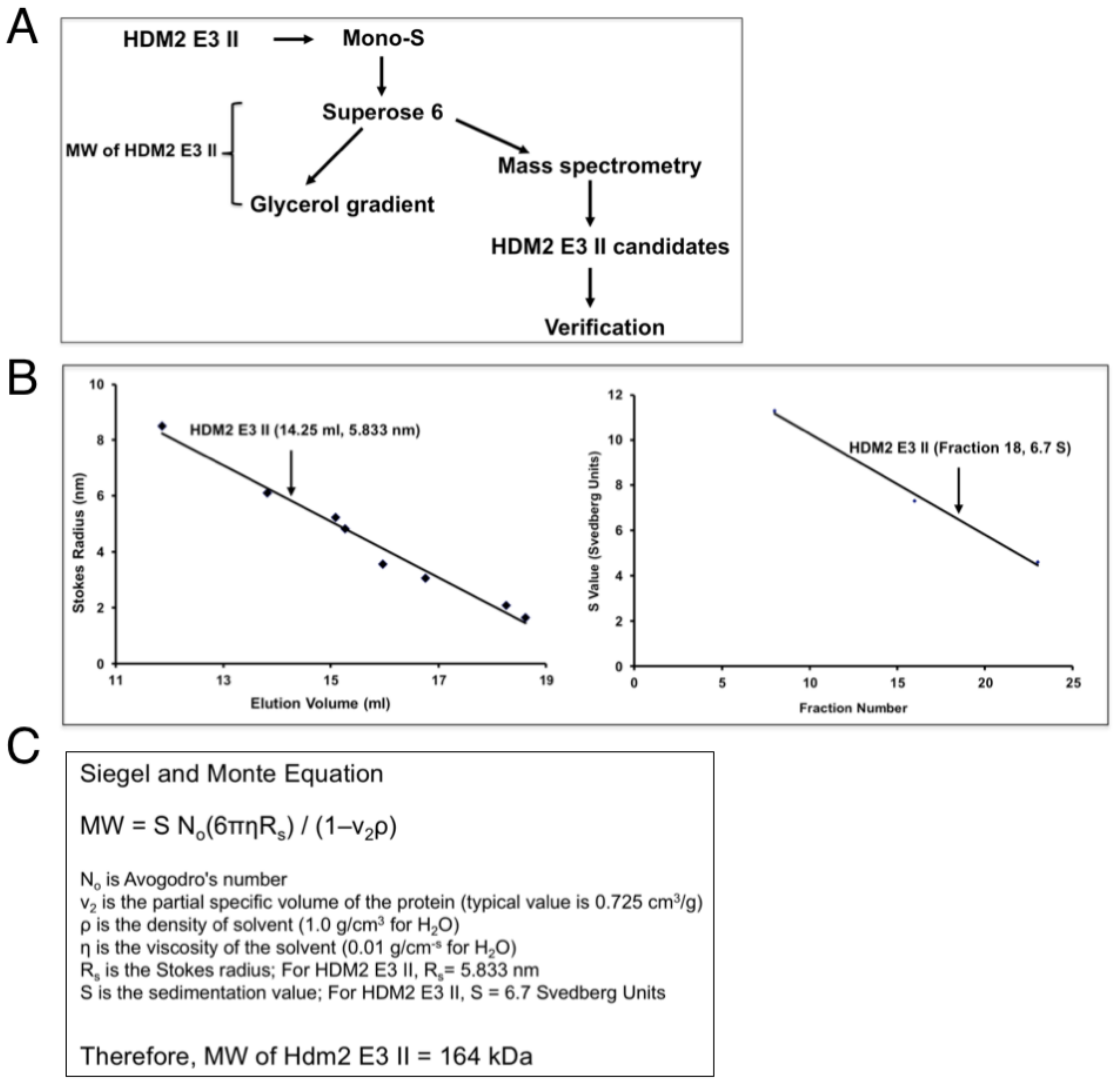


**Figure S2:** To purify HDM2 E3 II, we developed a procedure as diagrammed in panel A. Mono Q fractions containing HDM2 E3 II peak activity were pooled and further purified through mono S-based ion exchange, followed by sizing chromatography including Superose 6 and then glycerol gradient. In panel B, gel filtration by Superose 6 and density sedimentation by glycerol gradient determined the Stokes radius and S value of HDM2 E3 II: 5.833nm and 6.7S, respectively. Panel C shows calculation by applying Stokes radius and S value to the formula of Siegel and Monty[8], yielding HDM2 E3 II's apparent molecular weight: 164KDa.

A

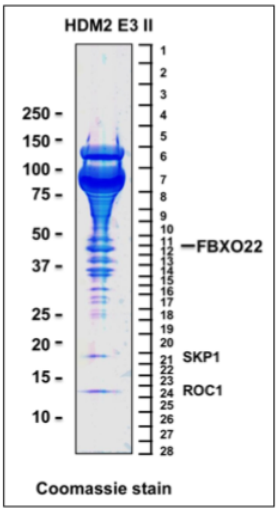


B

A partial list of E3 components present in the HDM2 E3 II fraction as identified by mass spectrometry

| Rank | Num Unique | Peptide Count | % Cov | Best Disc Score | Best Expect Val | Protein Length | Protein MW | Protein Name |
|---|---|---|---|---|---|---|---|---|
| [3] | 69 | 348 | 58.5 | 6.54 | 5.3E_10 | 776 | 89679.3 | Cullin_1 |
| [62] | 23 | 40 | 28.5 | 5.09 | 0.000000014 | 745 | 86983.9 | Cullin_2 |
| [56] | 20 | 21 | 30.6 | 6.03 | 3.4E_09 | 768 | 88931 | Cullin_3 |
| [13_1] | 28 | 70 | 34.7 | 3.84 | 0.00000034 | 759 | 87681 | Cullin_4A |
| [13] | 42 | 122 | 41.8 | 5.46 | 0.000000048 | 913 | 1039826 | Cullin_4B |
| [74] | 23 | 28 | 36 | 3.77 | 0.0000032 | 780 | 90956.2 | Cullin_5 |
| [75] | 16 | 129 | 73.6 | 5.12 | 0.000000076 | 163 | 18658.2 | Sphase kinase_associated protein 1 |
| [54] | 20 | 187 | 44.4 | 5.84 | 9.8E_10 | 403 | 44508.8 | F_box only protein 22 |
| [192] | 6 | 7 | 16.8 | 4.89 | 0.00000012 | 471 | 54561 | F_box only protein 3 |
| [351] | 3 | 3 | 8.8 | 3.5 | 0.00000039 | 522 | 58503.3 | F_box only protein 7 |
| [278] | 5 | 9 | 12 | 3.01 | 0.000015 | 300 | 32998.5 | F_box/LRR_repeat protein 15 |
| [236] | 4 | 31 | 18.5 | 5.36 | 5.1E_09 | 108 | 12274.1 | E3 ubiquitin_protein ligase RBX1 |
| | | | | | MW of $SCF^{FBXO22}$ | | 165120.4 | |

**Figure S3: Identification of $SCF^{FBXO22}$ as HDM2 E3 II.** *A) Coomassie stain of HDM2 E3 II fraction.* Superose 6 fraction #27, containing peak HDM2 E3 II activity (~4mg), was electrophoresed by 4-20% SDS-PAGE and separated protein bands were visualized by Coomassie staining. The entire gel slice was excised into 28 pieces that were subjected to mass spectrometry analysis. Piece #11 contains FBXO22. *B) A partial list of E3 components identified by mass spectrometry*. As highlighted, the number of unique peptides identified for $SCF^{FBXO22}$ is as follows: CUL1 (69), FBXO22 (20), Skp1 (16) and ROC1/Rbx1 (4). This complex is the most dominating E3 in the HDM2 E3 II fraction as identified by mass spectrometry. *C) Silver stain of purified $SCF^{FBXO22}$.*

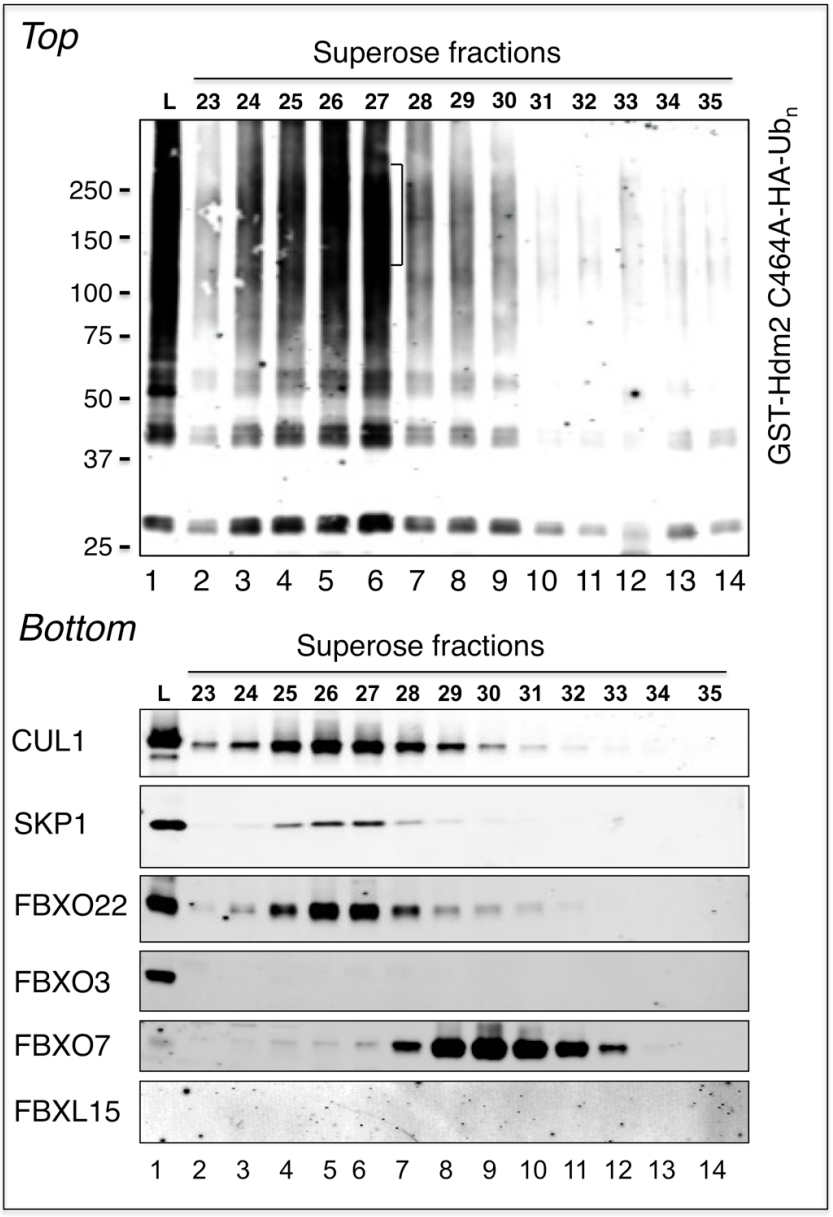


**Figure S4: Superose 6 fraction analysis of HDM2 E3 II.** *Top:* Aliquots of the indicated Superose 6 fraction (1µl) were assayed for E3 activity to support the ubiquitination of GST-HDM2 C464A. *Bottom:* Aliquots of the indicated Superose 6 fraction (5µl) were subjected to immunoblot analyses using antibodies as indicated.

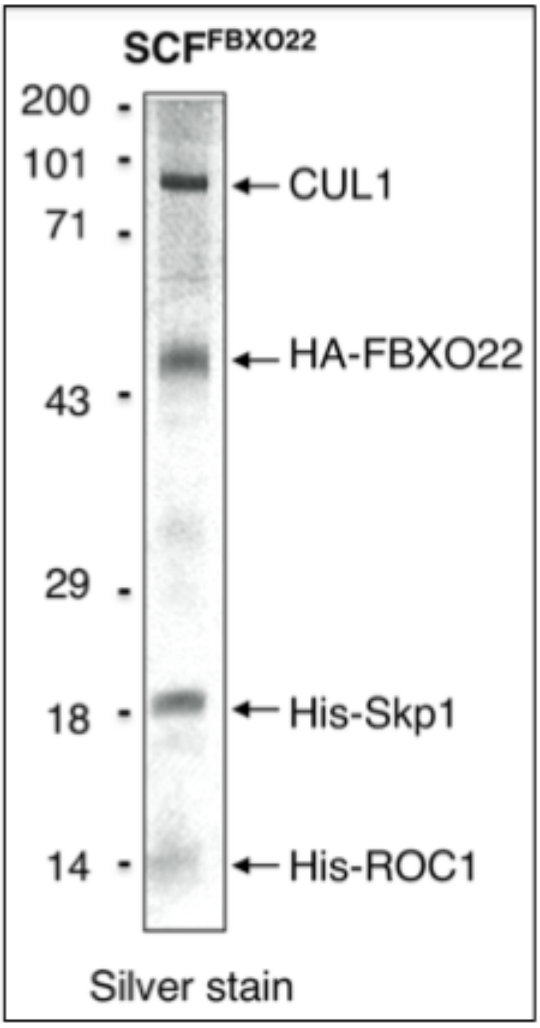


**Figure S5: Silver stain of purified $SCF^{FBXO22}$.**

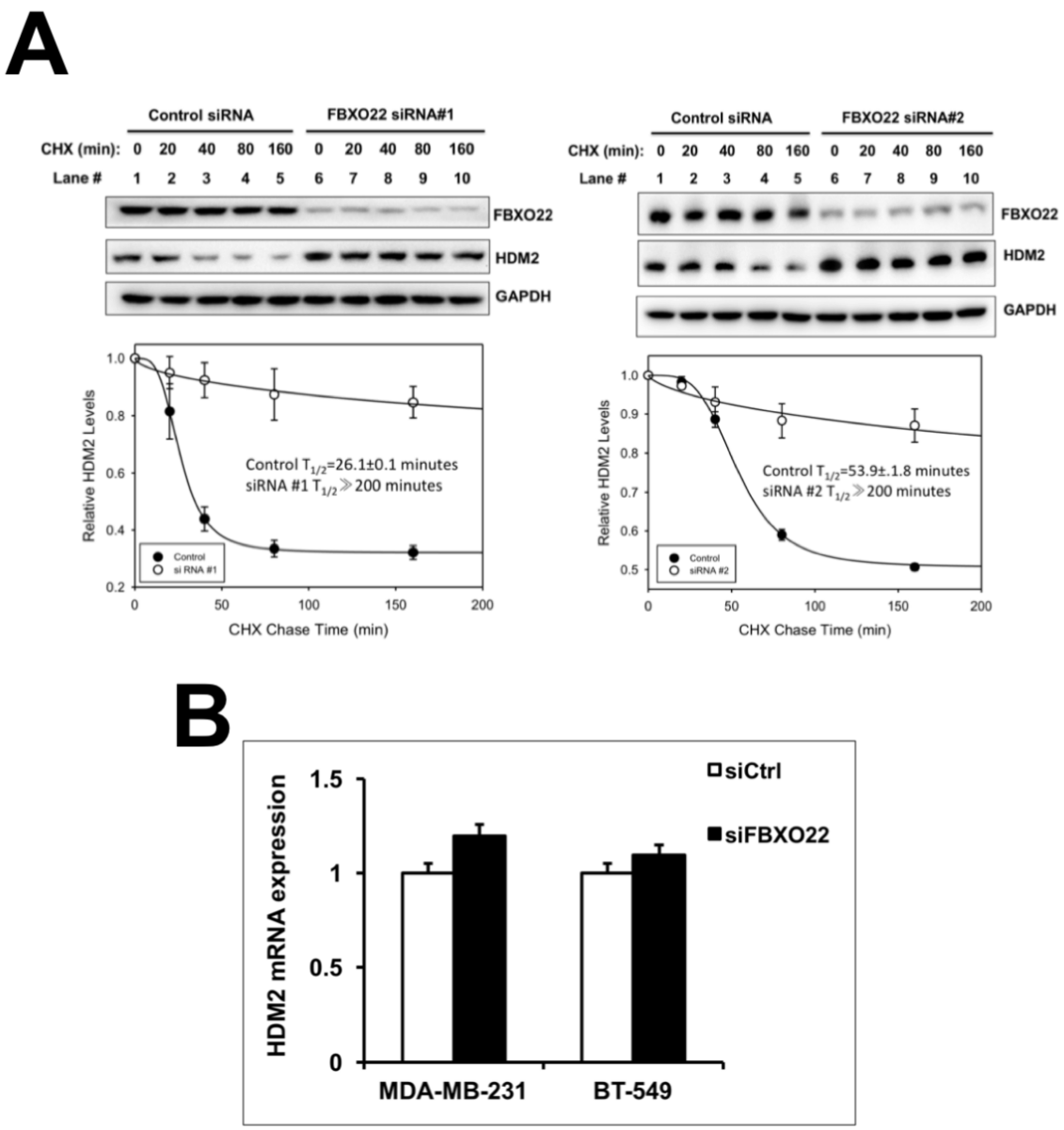


**Figure S6:** *A) Depletion of FBXO22 results in prolonged half-life of HDM2 in MDA-MB-231*. Cycloheximide assays were performed to measure HDM2 decay rates in cells treated with control or single FBXO22 KD siRNA#1 or #2. Graphs represent an average of three independent experiments (biological replicates), with error bars for SD. Graphing and calculation of the half-life ($T_{1/2}$) were done using the Scientific Data Analysis and Graphing Software SigmaPlot. *B) RT-PCR results show only slight effect of FBXO22 KD on HDM2 mRNA levels.* RNA from cells and tissues was extracted using

TRIzol Reagent (Thermo Fisher Scientific). cDNA was generated with random primers (Promega) using the Reverse Transcription System (Promega). Real-time PCR was carried out on ABI-7500 using SYBR Green Real-time PCR Master Mix (Vazyme Biotech, Nanjing, China). GAPDH was used for normalization of qRT-PCR data. Primer sequences are as follows: 1) GAPDH, forward, 5'-AAGGTCGGAGTCAACGGATTTG-3'; reverse, 5'-CCATGGGTGGAATCATATTGGAA-3'; 2) HDM2, forward, 5'-GCAAATGTGCAAT ACCAACATGTC-3'; reverse, 5'-GCCAAACAAATCTCCTAGAAGATC-3'.

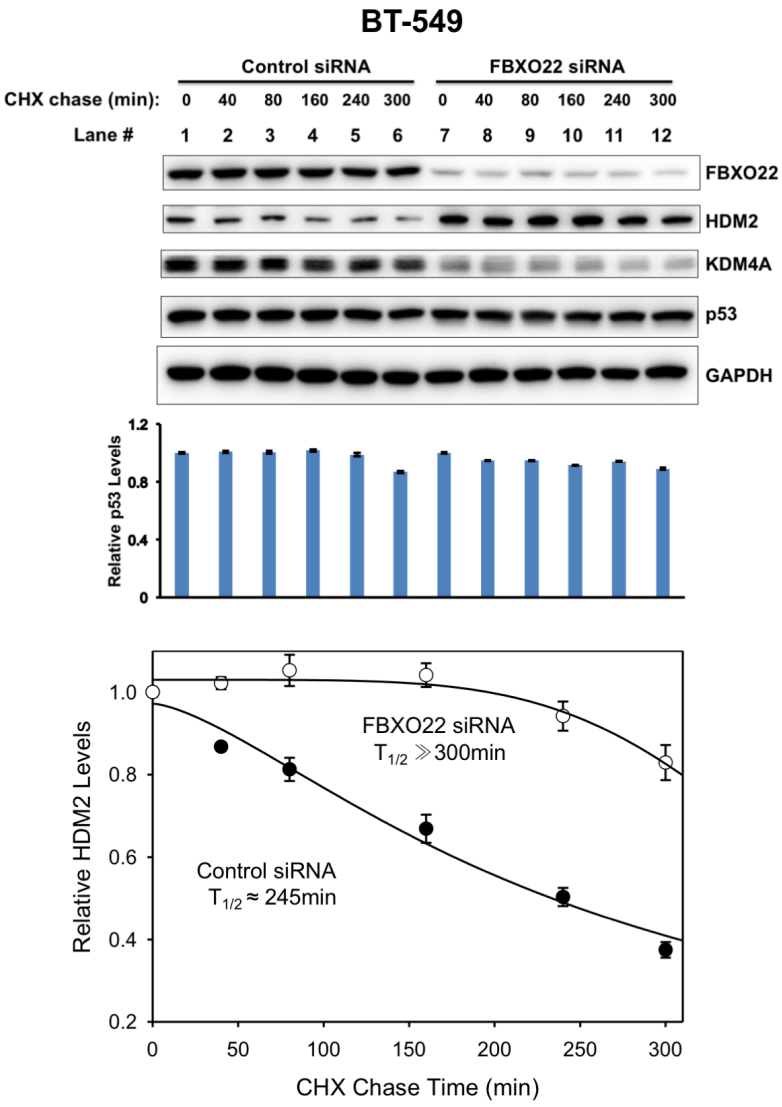


**Figure S7:** *Depletion of FBXO22 results in prolonged half-life of HDM2 in BT-549 cells*. Cycloheximide assays were performed to measure HDM2 decay rates in cells treated with control or FBXO22 KD siRNA. Graphs represent an average of three independent experiments (biological replicates), with error bars for SD. Graphing and calculation of the half-life ($T_{1/2}$) were done using the Scientific Data Analysis and Graphing Software SigmaPlot.

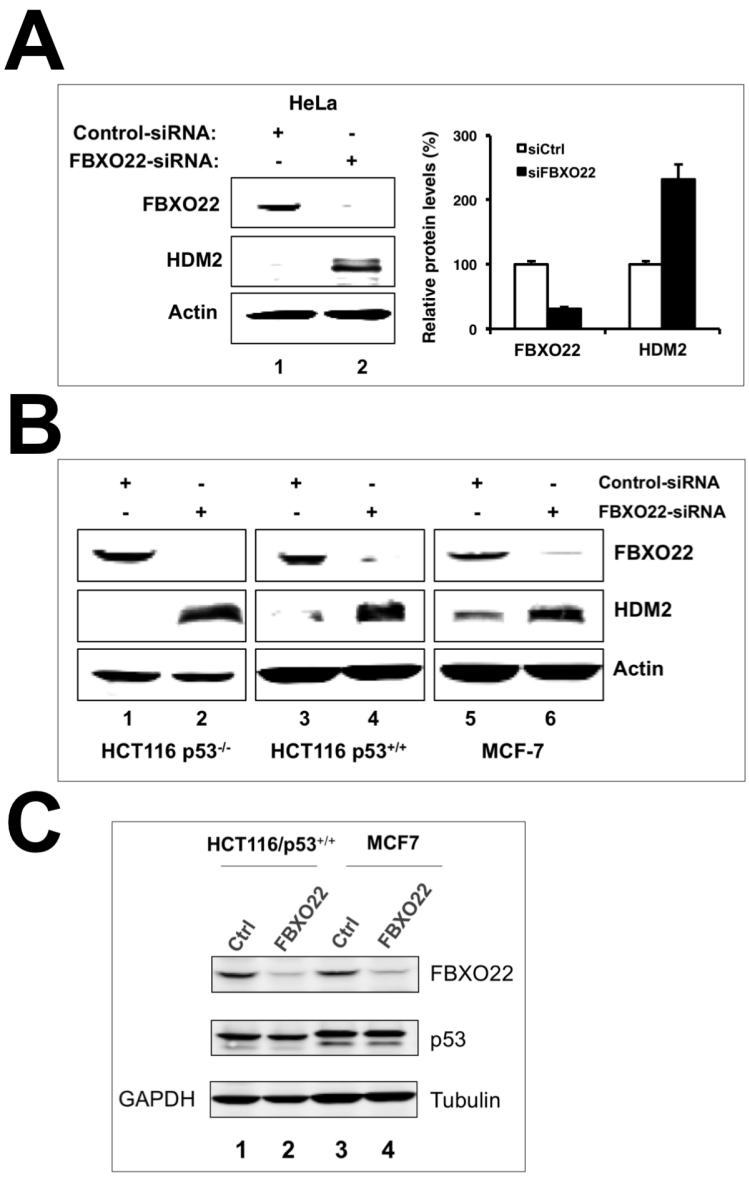


**Figure S8:** *A & B) Depletion of FBXO22 increased the protein level of HDM2.* Immunoblot analysis of the relative protein level of FBXO22 and HDM2 in indicated cell lines treated with siRNA against FBXO22 or with control siRNA. Data shown in panel A is quantified, expressing as mean ± standard deviation. *C) Effects of FBXO22 KD on p53 levels in HCT116 and MCF7 tumor cell lines.* Immunoblot analysis of the relative protein level of FBXO22 and HDM2 in indicated cell lines treated with siRNA against FBXO22.

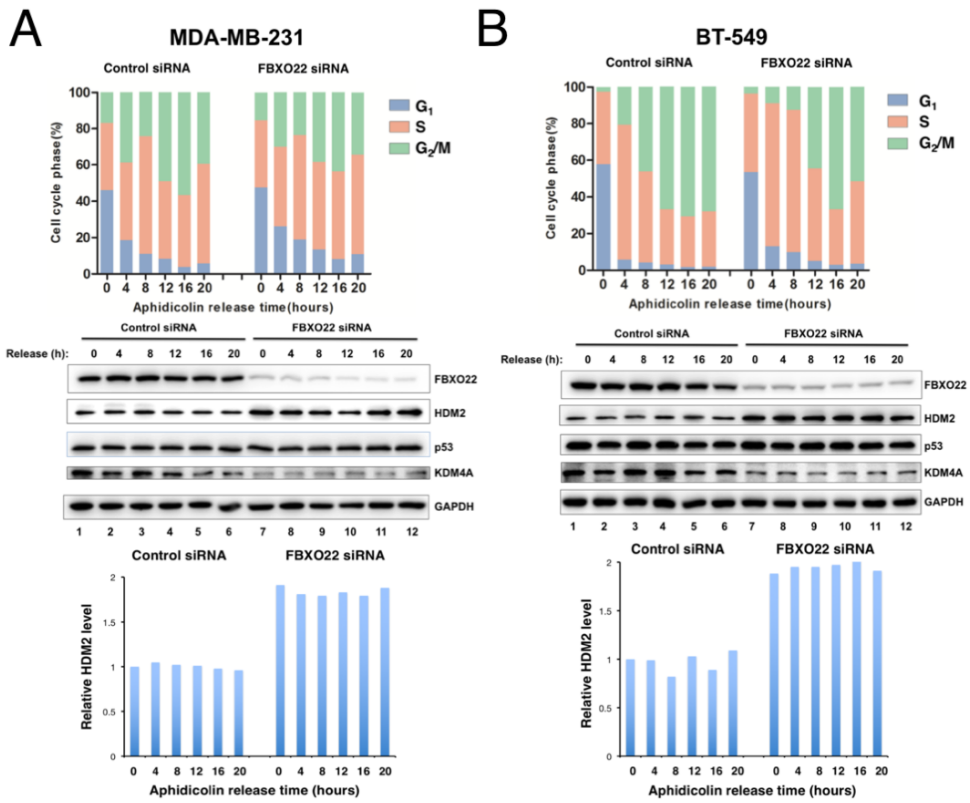


**Figure S9: FBXO22 targets HDM2 for degradation independently of cell cycle progression.** We examined the impact of FBXO22 KD in HDM2 levels during progression of the cell cycle. MDA-MB-231 or BT-549 cells treated with or without anti-FBXO22 siRNA were synchronized at $G_1$ and then allowed to enter cell cycle for times as indicated with the longest duration of 20 hours that were sufficient to complete one cycle. These samples were subjected to propidium iodide flow cytometry for cell cycle distribution, or immunoblot analysis for monitoring HDM2 levels.

Specifically, MDA-MB-231 or BT-549 cells were placed at a density of $10^6$ per 6cm diameter dish, allowed to adhere overnight. The cells were transfected with control siRNA or siRNA against FBXO22 at a concentration of 20nM. At 36h post-transfection, the resulting cells were treated with aphidicolin (Abcam) at a final concentration of 1μg/ml. At 12h post-treatment, the aphidicolin-containing medium was removed, and the cells were washed with phosphate buffered saline (PBS) and incubated in fresh medium

containing nocodazole (Selleckchem) (50ng/ml) for the indicated time. For flow cytometry analysis, the cells were fixed with 70% ethanol at 4°C overnight and stained with propidium iodide (KeyGEN BioTECH) at a concentration of 40μg/mL in hypotonic fluorochrome buffer (0.1% Triton X-100, 0.1% sodium citrate, and RNase A [25μg/ml]) for 30min. Samples were then subjected to flow cytometry analysis using a FACS Canto II flow cytometer (BD Biosciences).

Note that in either MDA-MB-231 or BT-549 cells, p53 levels remained unaltered throughout cell cycle in the presence of either control or FBXO22 siRNA. KDM4A levels varied during cell cycle. Consistent with observations shown in Fig. 2A, FBXO22 KD decreased KDM4A and this reduction effect was detected in all cell cycle phases (*middle*: compare lanes 1-6 and 7-12). The significance and mechanism for altered expression of KDM4A in cell cycle and the reduction effect by FBXO22 are presently unclear.

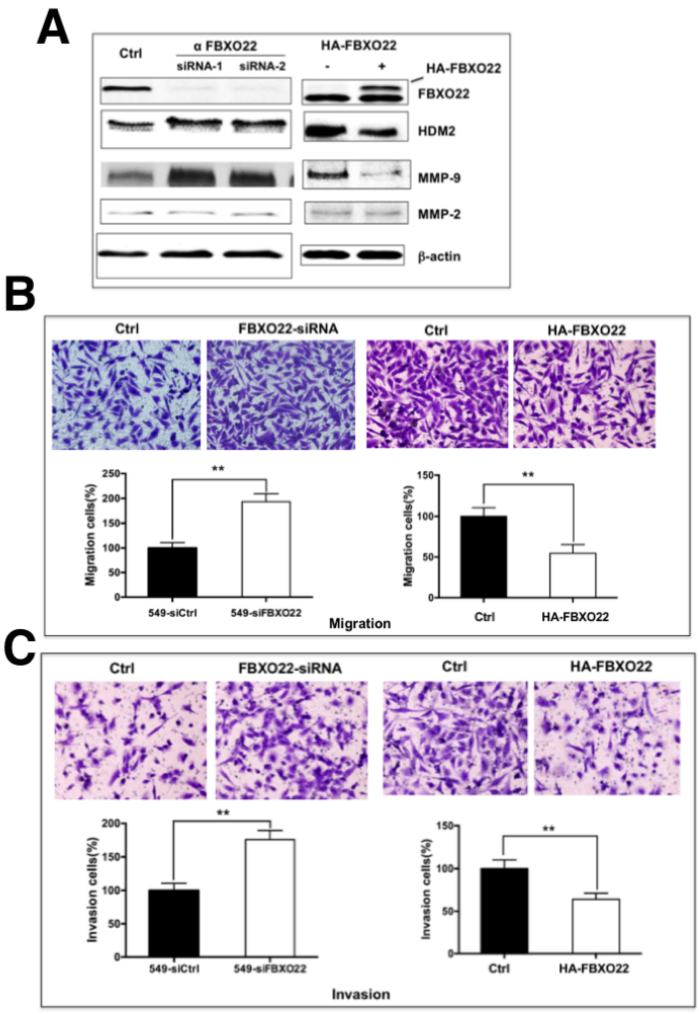


**Figure S10: FBXO22 inhibits migration and invasion of breast cancer cell line BT-549.** *A) Immunoblot analyses to confirm depletion of FBXO22 by siRNA and over-expression of FBXO22 by transfection. B) Effects on cell migration by depletion or overexpression of FBXO22. B) Effects on cell invasion by depletion or overexpression of FBXO22.* Data are shown as means ± SD (three biological replicates). **, $P < 0.01$.

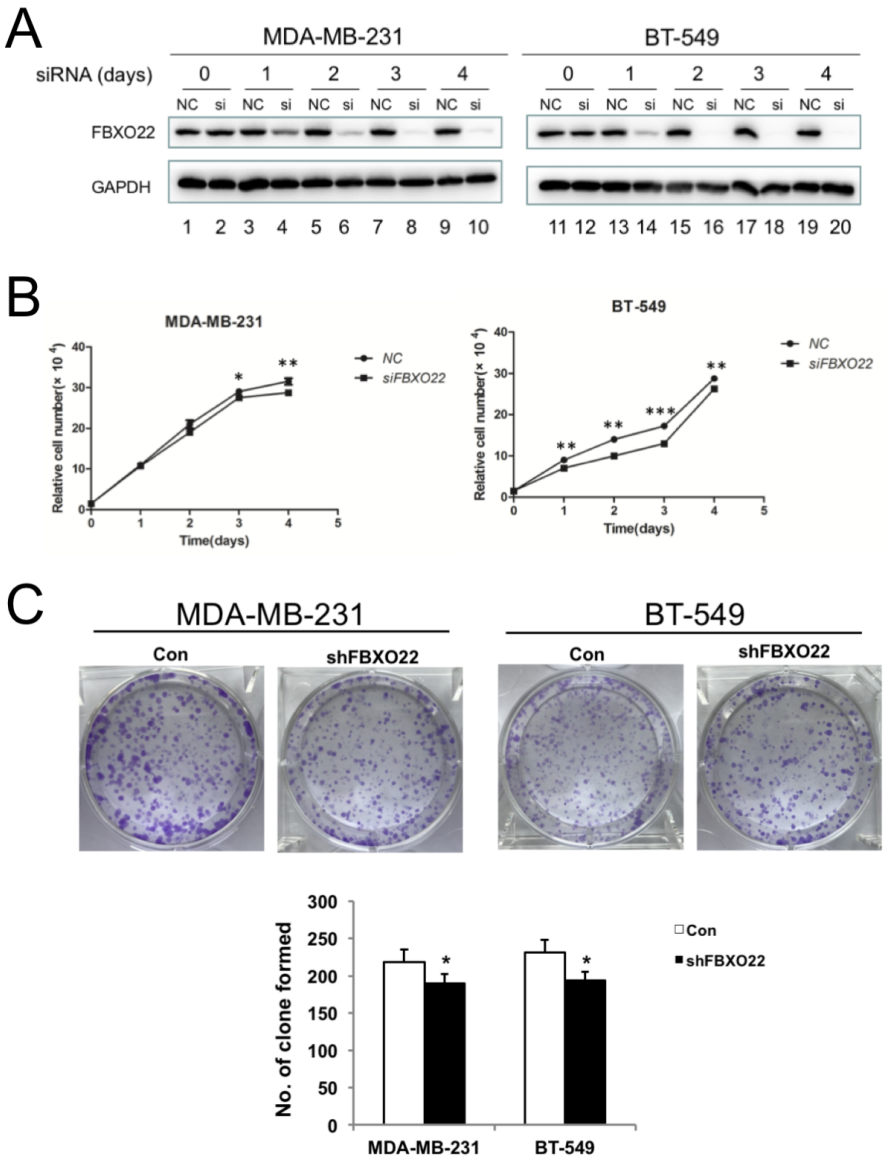


**Figure S11: FBXO22 KD has small inhibitory effects on proliferation and clonogenic survival of MDA-MB-231 and BT-549 breast cancer cells. A-B) Effects on growth**. MDA-MB-231 or BT-549 cells were placed at a density of $10^6$ per 6cm diameter dish, allowed to adhere overnight. The cells were transfected with control siRNA or siRNA against FBXO22 at a concentration of 20nM. At 12h post-transfection, the treated cells were processed as described below. re-plated at a density of $10^5$ per 3.5cm diameter dish and allow to grow for times as indicated. Immunoblot analysis was

performed to confirm depletion of FBXO22 by siRNA (panel **A**). To determine the effects on growth, the treated cells were re-plated at a density of $10^5$ per 3.5cm diameter dish and allow to grow for times as indicated. The cell numbers were counted at indicated time using Innovatis Cedex XS cell counter analyzer (Roche German), and shown in panel **B**). The culture medium was refreshed daily. **C) Clonogenic survival assay.** Cells were infected with lentivirus expressing control shRNA or shRNA against FBXO22 (sh-599). Note that the sh-599 targeted sequence in mouse and human is identical. The depletion of FBXO22 by sh-599 was confirmed (Fig. 5A). The shRNA-treated cells in a number of 1,000 were re-seeded into a new 6 well plates (in triplicate) and incubated for 14 days, during which culture media were changed every 5 days. The plates were washed twice with PBS, fixed with 90% methanol for 20min at -20°C and stained with crystal violet. Colonies was counted visually.

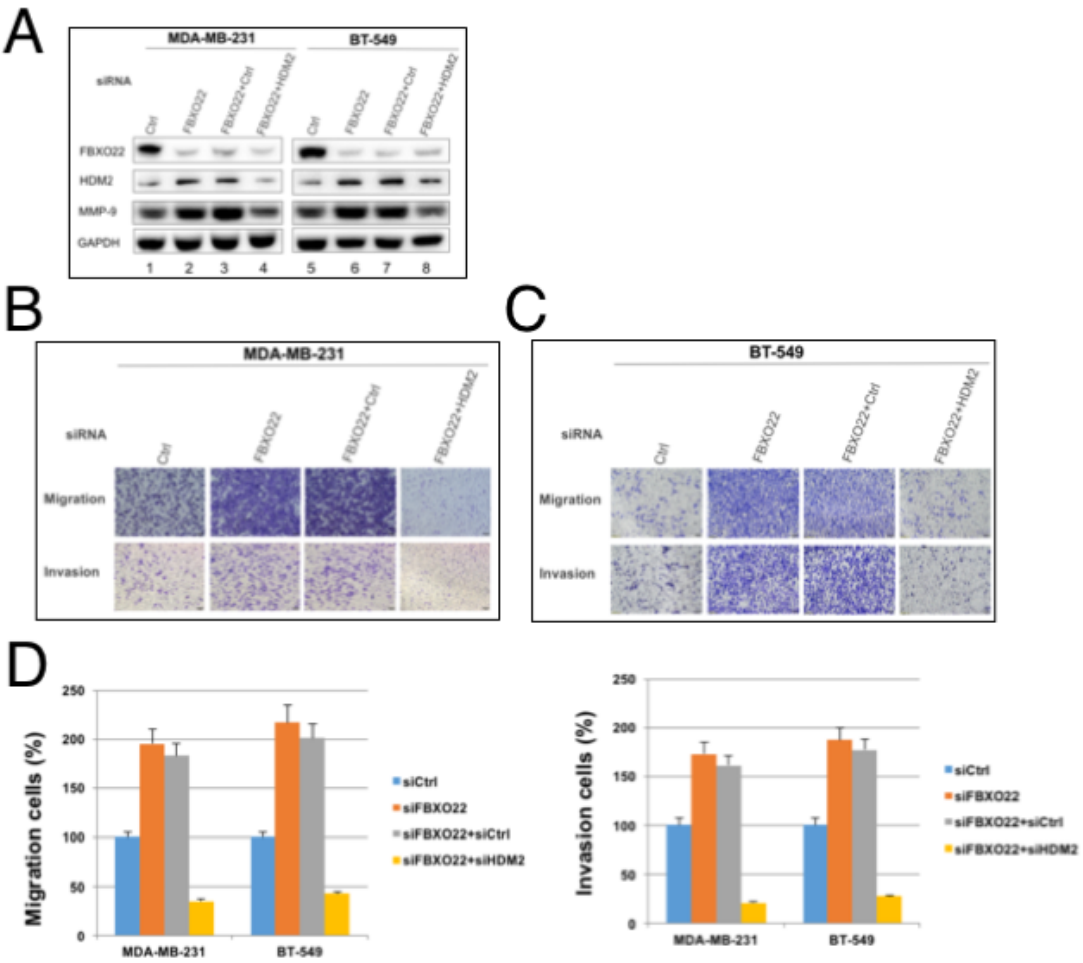


**Figure S12: FBXO22/HDM2 double KD suppresses the ability of FBXO22 KD cells to promote cell migration and invasion.** MDA-MB-231 or BT-549 cells were placed at a density of $10^6$ per 6cm diameter dish, allowed to adhere overnight. The cells were transfected with control siRNA (20nM), FBXO22 siRNA (20nM); FBXO22 siRNA (20nM) plus control siRNA (20nM); or FBXO22 siRNA (20nM) plus HDM2 siRNA (20nM). At 48h post-transfection, the treated cells were subjected to immunoblot analysis (panel A), or cell migration and invasion assays (Panel B-C). Quantification for panels B and C is shown in panel D. Note that the quantification for MDA-MB-231 cells is duplicated in Fig. 4D.

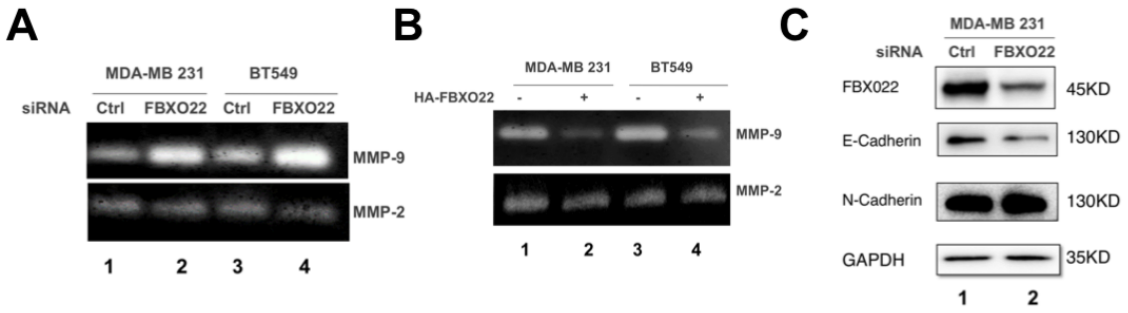


**Figure S13: A & B) FBXO22 suppressed MMP-9 activity in breast cancer cells.** A) Gelatin zymography analysis of the relative enzymatic activities of MMP-9 and MMP-2 in both MDA-MB-231 and BT-549 cell lines treated with siRNA. Gelatin zymography was performed as described before[9]. Thirty-six hours after transfection, cells were incubated in serum-free medium for 24h. The proteins in the conditioned medium were concentrated with Amicon Ultra-4-30K centrifugal filters (Millipore, MA, USA) at 7500Xg for 20min at 4°C. Fifty micrograms of the proteins were loaded on a 10% polyacrylamide gel containing 0.1% gelatin (Sigma, MO, USA). Gelatinolytic activity was shown as clear areas on the gel. Gels were photographed and then the signals were quantified by scanning densitometry. (B) Gelatin zymography analysis of the relative enzyme activities of MMP-9 and MMP-2 in both MDA-MB-231 and BT-549 cell lines transfected with FBXO22 over-expression vector. **C) FBXO22 knockdown reduced E-Cadherin expression in breast cancer cells.** MDA-MB-231 cells were treated with siRNA and then subjected to immunoblots analysis using antibodies as indicated.